Pergamon

Computers chem. Engng Vol. 19, No. 11, pp. 1207–1218, 1995

0098-1354(94)00117-0
0098-1354/95 $9.50 + 0.00

TRANSPORT EFFECTS IN PACKED-BED OXIDATION REACTORS

B. ROSENDALL and B. A. FINLAYSON
Department of Chemical Engineering, University of Washington, Seattle, WA 98195, U.S.A.

(Received 8 April 1994; final revision received 4 October 1994; received for publication 7 November 1994)

Abstract—Three gas-phase oxidation reactors are studied: the reaction of sulfur dioxide to sulfur trioxide, *o*-xylene to phthalic anhydride, and n-butane to maleic anhydride. Mathematical models are developed to account for the transport phenomena in packed-bed reactors. A software package, the Chemical Reactor Design Tool, is used to solve these models and assess the effect of transport phenomena. Phenomena studied include heat and mass transfer resistances around the catalyst particles; density, velocity, and pressure variations; radial dispersion; and axial dispersion. Criteria are developed and taken from the literature to estimate the importance of these phenomena *a priori*. These criteria are compared with the results of the computer simulations. In most cases, the criteria accurately predict which phenomena are important to a particular reactor design. When the estimate from the criterion is questionable or borderline, computer simulations can be used to investigate the phenomenon's significance.

INTRODUCTION

In most cases, mathematical models that accurately describe industrial reactors cannot be solved analytically. Gas-phase oxidation catalytic reactors with strong heat effects are no exception. Of the commonly used models, the most basic model is the plug-flow reactor that ignores heterogeneous effects, axial and radial dispersion, and density variations due to pressure, temperature, and mole changes. Ignoring these effects can often be justified by calculating certain critria before model development, but otherwise the effect should be included. For most gas-phase oxidation reactors, the model's result is a set of non-linear ordinary or partial differential equations that have no analytical solution. With the aid of a computer, a variety of numerical methods can be used to solve the model.

To investigate the many phenomena that are important in the design of chemical reactors, a set of computer codes has been developed. This Chemical Reactor Design Tool (CRDT; Finlayson *et al.*, 1995a, b) uses an X-Window environment to prompt the user for the required data for any particular design. The user supplies a FORTRAN subroutine that contains information about reaction rates. Complex, multiple-reaction systems are easily included. Reactor types that can be modeled with CRDT include:

(1) batch reactors
(2) continuous stirred-tank reactors (CSTR)
(3) plug-flow reactors (PFR)
(4) plug-flow reactors with axial dispersion (axial)
(5) tubular-flow reactors with radial dispersion (2-D reactor).

Many typical effects that are often ignored can be included separately with CRDT, thus enabling the user to study each effect individually. These effects include heterogeneous effects, dispersion due to catalyst packing, and density and velocity variation due to pressure drop, heat effects, and mole changes from reaction. The significance of ignoring each phenomenon can be easily determined by selecting the appropriate option, usually by clicking a button, and providing a few additional parameters. The CRDT then selects the appropriate numerical tool and solves the equations.

The CRDT is used to study three gas-phase oxidation reactors:

(1) oxidation of sulfur dioxide to sulfur trioxide, extending Young and Finlayson (1973);
(2) oxidation of *o*-xylene to phthalic anhydride, extending Froment and Bischoff (1990); and
(3) oxidation of n-butane to maleic anhydride, extending Sharma *et al.* (1991).

The CRDT allows the user to include effects ignored in the original studies; Table 1 summarizes the effects included by the previous investigators. Criteria are developed or taken from literature to estimate the importance of various phenomena, including:

(1) heterogeneous effects

Table 1. Importance of phenomena from the literature

Phenomenon	Sulfur trioxide	Phthalic anhydride	Maleic anhydride
Radial dispersion	Yes	Yes	Maybe
Axial dispersion	Yes	No	No
Heterogeneity	Yes	No	Yes
Density variations	No	No	No

(2) density variation
(3) radial dispersion
(4) axial dispersion.

The criteria's reliability is determined by comparing the results from CRDT with the results from the original studies.

MODELS AND METHODS

The model for the PFR is derived from the steady-state continuity equation for species j and from the steady-state energy balance assuming that convective transport dominates over diffusive transport. The energy balance includes the removal of energy at the wall. The velocity is assumed constant across the cross-section of the reactor, but can vary in the axial direction. The result is shown in equations (1) and (2) along with the appropriate inlet condition:

$$\frac{dF_j}{dV} = \rho_B R_j \quad j = 1, \ldots, N \tag{1}$$

$$\sum_{j=1}^{N} F_j C_{pj} \frac{dT}{dV} = \rho_B \sum_{i=1}^{M} (-\Delta H_{rxn,i}) r_i - \frac{4U}{d_t}(T - T_a). \tag{2}$$

Inlet conditions:

$$F_j(V=0) = F_{j0}, \quad T(V=0) = T_0.$$

The rate of consumption or production of species j is given in equation (3):

$$R_j = \sum_{i=1}^{M} v_{ji} r_i, \tag{3}$$

where v_{ji} is the stoichiometric coefficient of species j in reaction i (+ for products, − for reactants) and r_i is the rate expression for reaction i.

Note that these equations are coupled not only through the reaction rate term but also through the heat capacity term, which includes molar flow rates. Both molar flow rates and concentrations or partial pressures appear in these equations because the rate expressions are usually functions of concentrations or partial pressures. Any necessary conversion between moles, concentration, and/or partial pressures is automatic within the program. For gas-phase reactors, the conversion uses the ideal gas law. The CRDT can solve these equations with three different ordinary differential equation integration routines: a second- or fourth-order Runge–Kutta method (RKF45) or an automatic time-stepping implicit integration routine (LSODE, Hindmarsh, 1983).

Equations (4) and (5) describe the PFR with axial dispersion:

$$\varepsilon D_{ea} \frac{d^2 C_j}{dz^2} - \frac{d(uC_j)}{dz} + \rho_B R_j = 0 \quad j = 1, \ldots, N \tag{4}$$

$$\lambda_{ea} \frac{d^2 T}{dz^2} - u \sum_{j=1}^{N} C_j C_{pj} \frac{dT}{dz} + \rho_B \sum_{i=1}^{M} (-\Delta H_{rxn,i}) r_i - \frac{4U}{d_t}(T - T_w) = 0. \tag{5}$$

Boundary conditions at $z = 0$:

$$-\varepsilon D_{ea} \frac{dC_j}{dz} = u_0 C_{j,0} - u(0) C_j(0)$$

$$-\lambda_{ea} \frac{dT}{dz} = u \sum_{j=1}^{N} C_j C_{pj} [T_0 - T(0)],$$

at $z = L$:

$$\frac{dC_j}{dz} = 0 \quad \frac{dT}{dz} = 0.$$

Derivation of these equations is similar to the PFR, except that this model includes diffusive transport in the axial direction. Danckwerts boundary conditions are applied at the inlet (Froment and Bischoff, 1990). To solve equations (4) and (5), CRDT gives users a choice between the finite difference method and the orthogonal collocation method. These methods give large sets of non-linear equations, which are solved using the Newton–Raphson method. An initial guess is determined using linear programming to deduce the maximum and minimum temperature. For the orthogonal collocation method, if convergence fails a homotopy method is used (Seader, 1985).

Equations (6) and (7) show the model for the 2-D reactor:

$$\frac{1}{A_c} \frac{\partial F_j}{\partial z} - \varepsilon D_{er} \left(\frac{\partial^2 C_j}{\partial r^2} + \frac{1}{r} \frac{\partial C_j}{\partial r} \right) + \rho_B R_j = 0 \quad j = 1, \ldots, N \tag{6}$$

$$\frac{1}{A_c} \sum_{j=1}^{N} F_j C_{pj} \frac{\partial T}{\partial z} - \lambda_{er} \left(\frac{\partial^2 T}{\partial r^2} + \frac{1}{r} \frac{\partial T}{\partial r} \right) + \rho_B \sum_{i=1}^{M} (-\Delta H_{rxn,i}) r_i = 0. \tag{7}$$

Inlet conditions:

$$F_j(z=0)=F_{j0},\quad T(z=0)=T_0.$$

Boundary conditions at $r=0$:

$$\frac{dC_j}{dr}=0\quad\frac{dT}{dr}=0,$$

at $r=1$:

$$\varepsilon D_{er}\frac{\partial C}{\partial r}=0$$

$$\lambda_{er}\frac{\partial T}{dz}=h_w(T-T_w).$$

This model includes diffusive transport in the radial direction but not in the axial direction. Also, the assumption of plug flow is relaxed. The CRDT allows for a radial variation in the axial velocity, and solves equations (6) and (7) using either the finite difference method or the orthogonal collocation method. These methods reduce the set of partial differential equations to a larger set of ordinary differential equations, which are solved using the same methods applied to the plug-flow model.

To compare the 2-D model to the 1-D models, the wall heat transfer coefficient, h_w, needs to be correlated to the overall heat transfer coefficient, U. For the sulfur trioxide and maleic anhydride reactors, the relationship from Young and Finlayson (1973) is used:

$$\frac{1}{U}=\frac{1}{h_w}+\frac{R_t}{3\lambda_{er}}. \tag{8}$$

For the phthalic anhydride reactor, Froment and Bischoff (1990) give the following equation:

$$\frac{1}{U}=\frac{1}{h_w}+\frac{R_t}{4\lambda_{er}}. \tag{9}$$

For all these models, the total concentration (density) can be assumed constant, or it can vary due to temperature, pressure, and/or mole changes due to reaction. When the density varies, the velocity also varies to satisfy the continuity equation:

$$\rho u A_c=\text{constant}. \tag{10}$$

Heterogeneous effects require the reaction rate to be evaluated at the concentrations and temperature at the catalyst's surface. For mass and heat transfer resistances external to the catalyst, the reaction rates, along with the surface concentrations and temperature, are determined by solving the set of algebraic equations given in equations (11) and (12):

$$k_m a(C_j-C_{s,j})=-\rho_B R_j(C_s,T_s) \tag{11}$$

$$h_p a(T-T_s)=-\rho_B\sum_{i=1}^{M}(\Delta H_{rxn,i})r_i(C_s,T_s). \tag{12}$$

This set of non-linear algebraic equations is solved with the Newton–Raphson method. A homotopy method is employed if the Newton–Raphson method does not converge. For both methods, the initial guess is obtained by determining the maximum possible temperature with linear programming methods. The reaction rate routine uses effectiveness factors to account for mass and heat transfer resistances internal to the catalyst.

The CRDT calculates the pressure drop with equation (13):

$$\frac{dP}{dz}=\left(\frac{dP}{dz}\right)_0\frac{u}{u_0}. \tag{13}$$

Inlet condition:

$$P=P_0\quad\text{at}\quad z=0.$$

The inlet pressure gradient for the simulations presented here is calculated with the Ergun equation:

$$\left(\frac{dP}{dz}\right)_0=\frac{1-\varepsilon}{\varepsilon^3}\frac{\rho_0 u_0^2}{d_p}\left[\frac{150(1-\varepsilon)}{Re_p}+1.75\right]. \tag{14}$$

The user manuals for the Chemical Reactor Design Tool contain complete derivations of the models and methods (Finlayson *et al.*, 1995a, b).

SIMULATIONS

Presented here are the reaction systems and rate expressions for the three oxidation reactors investigated. The first is the oxidation of sulfur dioxide to sulfur trioxide with a platinum coated catalyst (Young and Finlayson, 1973):

$$SO_2+\tfrac{1}{2}O_2\rightarrow SO_3 \qquad \text{RXN 1}$$

$$r_1=\frac{X\sqrt{1-0.166(1-X)}-2.2(1-X)/K_{eq}}{(k_1+k_2(1-X))^2}$$

$$[=]\frac{\text{kmol}}{\text{kgcat.hr}}$$

$$k_1=\exp\left(-14.96+\frac{11070}{T(\text{K})}\right)$$

$$k_2=\exp\left(-1.331+\frac{2331}{T(\text{K})}\right)$$

$$K_{eq}=\exp\left(-11.02+\frac{11570}{T(\text{K})}\right)$$

$$\Delta H_{rxn,1}=-97{,}500\ \text{kJ/kmol}. \tag{15}$$

The second reaction system studied is the oxidation of *o*-xylene over V_2O_5 catalysts (Froment and Bischoff, 1990):

$$C_8H_{10} + 3O_2 \rightarrow C_8H_4O_3 + 3H_2O \quad \text{RXN 2}$$

$$C_8H_4O_3 + \tfrac{15}{2}O_2 \rightarrow 8CO_2 + 2H_2O \quad \text{RXN 3}$$

$$C_8H_{10} + \tfrac{21}{2}O_2 \rightarrow 8CO_2 + 5H_2O \quad \text{RXN 4}$$

$$r_1 = k_1 p_{oxy} p_{o_2} [=] \frac{\text{kmol}}{\text{kgcat.hr}}$$

$$\Delta H_{rxn,1} = 1{,}285{,}000 \text{ kJ/kmol}$$

$$r_2 = k_2 p_{pa} p_{o_2}$$

$$\Delta H_{rxn,2} = 3{,}279{,}000 \text{ kJ/kmol}$$

$$r_3 = k_3 p_{oxy} p_{o_2}$$

$$\Delta H_{rxn,3} = 4{,}564{,}000 \text{ kJ/kmol}$$

$$k_1 = \exp\left(19.837 - \frac{13588}{T(\text{K})}\right)$$

$$k_2 = \exp\left(20.86 - \frac{15803}{T(\text{K})}\right)$$

$$k_3 = \exp\left(18.97 - \frac{14394}{T(\text{K})}\right). \quad (16)$$

The third study is the oxidation of n-butane to maleic anhydride with a vanadium–phosphor oxide catalyst (Sharma *et al.*, 1991):

$$C_4H_{10} + \tfrac{7}{2}O_2 \rightarrow C_4H_2O_3 + 4H_2O \quad \text{RXN 5}$$

$$C_4H_2O_3 + O_2 \rightarrow 4CO + H_2O \quad \text{RXN 6}$$

$$C_4H_{10} + \tfrac{11}{2}O_2 \rightarrow 2CO + 2CO_2 + 5H_2O \quad \text{RXN 7}$$

$$r_1 = \frac{k_1 p_{but}^{0.54}}{1 + 310 p_{ma}} [=] \frac{\text{kmol}}{\text{kgcat.s}}$$

$$\Delta H_{rxn,1} = 1{,}239{,}000 \text{ kJ/kmol}$$

$$r_2 = \frac{k_2 p_{ma}}{(1 + 310 p_{ma})}$$

$$\Delta H_{rxn,2} = 281{,}000 \text{ kJ/kmol}$$

$$r_3 = k_3 p_{but}^{0.54}$$

$$\Delta H_{rxn,3} = 2{,}087{,}000 \text{ kJ/kmol}$$

$$k_1 = 0.96 \times 10^{-6} \exp\left[\frac{93100}{673R}\left(1 - \frac{673}{T(\text{K})}\right)\right]$$

$$k_2 = 0.29 \times 10^{-5} \exp\left[\frac{155000}{673R}\left(1 - \frac{673}{T(\text{K})}\right)\right]$$

$$k_3 = 0.15 \times 10^{-6} \exp\left[\frac{93100}{673R}\left(1 - \frac{673}{T(\text{K})}\right)\right]. \quad (17)$$

Table 2. Parameters for simulations

Parameter	Sulfur trioxide	Phthalic anhydride	Maleic anhydride
L (m)	0.15	3.0	5.0
R_t (m)	0.026	0.0127	0.0125
d_p (m)	0.0032	0.003	0.003
ε	0.43	0.5	0.44
y_{ao}	0.065	0.00924	0.0186
T_o (K)	673	628	450
T_w (K)	470	628	663
P_o (atm)	1.0	1.0	1.65
G (kg/m^2 s)	0.475	1.3	1.25
Re	46	121	121
$Pe_{m,r}$	9.6	10	8
$Pe_{m,L}$	93.8	1000	1667
$k_{e,r}$ (kJ/ms K)	0.00049	0.00078	0.0011
$k_{e,z}$ (kJ/ms K)	0.0016	0.0034	0.0029
$Pe_{h,r}$	3.23	5.25	3.79
$Pe_{h,L}$	45.9	1210	2360
Bi	10	2.54	1.9
U_o (kJ/m^2 s K)	0.042	0.0845	0.104
St	1.02	29.0	61.0
Da_I	0.15	0.0078	0.00306
Da_{III}	0.70	0.516	0.205
ka (s^{-1})	186	74	—
ha (kJ/m^3 s K)	251	290	—
$dP/dz\|_o * L/P_o$	−0.005	−0.054	−0.19

Table 2 lists the parameters used in these models.

Ten simulations were run for each of the three reaction systems. Table 3 lists the cases run. The heterogeneous effects in the simulations represent mass and heat transfer resistances external to the catalyst for the sulfur trioxide and phthalic anhydride reactors. For the maleic anhydride reactor, the resistances are internal to the catalyst and the effectiveness factors are provided by previous investigators. The heat and mass transfer coefficients for the sulfur trioxide reactor were also given by Young and Finlayson (1973). The mass and heat transfer coefficients for the phthalic anhydride reactor were calculated using correlations from literature (Froment and Bischoff, 1990).

Relative computation time for each of these 10 simulations strongly depends on the problem. A simulation for the axial diffusion problem usually requires more CPU time than a simple PFR problem. This is because of the nature of the numerical solution. The axial diffusion problem is a boundary

Table 3. Simulations

1	PFR—Total concentration constant—homogeneous
2	PFR—Total concentration varies—homogeneous
3	PFR—Total concentration constant—heterogeneous
4	PFR—Total concentration varies—heterogeneous
5	PFR with axial dispersion—total concentration constant—homogeneous
6	PFR with axial dispersion—total concentration varies—homogeneous
7	PFR with axial dispersion—total concentration constant—heterogeneous
8	PFR with axial dispersion—total concentration varies—heterogeneous
9	2-D reactor—total concentration constant—homogeneous
10	2-D reactor—total concentration constant—heterogeneous

value problem requiring the solution of large sets of coupled, non-linear algebraic equations. The PFR problem is an initial-value problem requiring numerical integration. A highly non-linear problem will require more CPU time. By contrast, if the problem is linear, the solution time for the axial diffusion problem can be less than a simple PFR problem.

The reactor problems with radial dispersion involve a set of partial differential equations, which combines a boundary value problem with an initial value problem. The solution requires numerical integration of N times more equations than the PFR problem, where N is the number of points in the radial direction.

Adding density variation to the problem results in an extra equation to solve in the PFR and 2-D problems. For the axial diffusion problem, the iterative procedure becomes a successive substitution method instead of the Newton–Raphson method because the velocity is evaluated at the last iteration. The error in the Newton–Raphson method is reduced quadratically whereas the successive substitution converges linearly. Thus, density variations will always increase the solution time for all problems, generally more so in the axial diffusion problem.

Solution time is increased greatly for heterogeneous problems where the resistance is external to the catalyst. This is because a set of algebraic equations must be solved every time the rate expression needs to be evaluated during the solution. The amount of added solution time depends on the number of times the rate needs to be evaluated. In general, the amount of added time is the least for the PFR model and the most for the axial diffusion problem. The axial diffusion model requires evaluation of the rate expression at every point in every iteration.

If the heterogeneous problem is for internal resistance, the solution time is negligibly increased because effectiveness factors are used in the rate expression. The only addition to the problem is the multiplication of the effectiveness factor and rate term. Table 4 illustrates the relative increase in CPU time for the phthalic anhydride reactor. Note that these values will change for different reaction systems, but span a range of a factor of 50 for this case.

Table 4. Solution time for phthalic anhydride reaction system

Simulation	Relative CPU time
PFR	1.0
with density variations	1.1
with external resistance	2.3
Axial	1.5
with density variation	4.0
with external resistance	36.0
2-D	5.0
with external resistance	50.0

CRITERIA

A criterion for the importance of heterogeneity was developed by solving equation (1) assuming first-order kinetics for two cases: case 1 without heterogeneous effects and case 2 with heterogeneous effects. The solution of these equations gives outlet concentrations for the two cases shown in equations (18) and (19):

$$C_{a1} = C_{a0} \exp\left[\frac{\rho_B R_{a0} V}{F_{a0}}\right] \tag{18}$$

$$C_{a2} = C_{a0} \exp\left[\frac{\rho_B \eta R_{a0} V}{F_{a0}}\right]. \tag{19}$$

We take as the criterion that these concentrations should be within 1% of each other in order to ignore heterogeneous effects. Concentration variations greater than 1% could have a profound effect on the economics for large-scale production:

$$\left|\frac{C_{a2}}{C_{a1}} - 1\right| < 0.01. \tag{20}$$

Thus heterogeneous effects can be ignored if the effectiveness factor satisfies equation (21):

$$1 - \frac{0.01F_0}{\rho_B R_0 V} \leq \eta \leq 1 + \frac{0.01F_0}{\rho_B R_0 V}. \tag{21}$$

Development of a criterion for density variations is done in a similar manner. The equation for the PFR is solved twice assuming first-order kinetics. The first case assumes a constant velocity equal to the inlet velocity, $u_1 = u_0$. The second solution assumes a constant velocity equal to an estimated outlet velocity. The estimated outlet velocity is calculated using equation (22):

$$u_2 = u_1 \frac{T_w P_0}{T_0 P_L (1 + \varepsilon_a)} \tag{22}$$

T_w = wall temperature

$$P_L = P_0 - \left[\frac{dP}{dz}\right]_0 L$$

$$\varepsilon_a = y_{a0}\delta$$

$$\delta = \sum_{j=1}^{n} \frac{\nu_j}{\nu_a}.$$

We take as the criterion that the outlet concentra-

tion for case 1 varies from the outlet concentration for case 2 by less than 1%. Density variations can be ignored when equation (23) is satisfied:

$$1-\frac{0.01F_0}{\rho_B R_0 V}\leq\frac{u_1}{u_2}\leq 1+\frac{0.01F_0}{\rho_B R_0 V}. \tag{23}$$

Estimating the significance of radial dispersion is also done by solving the PFR equation for two cases. Temperature differences are the basis for this criterion because the major factor contributing to radial dispersion is a radial temperature profile caused by heating or cooling at the wall. The radial temperature gradient forces a concentration gradient through the temperature dependence of the rate expression. This criterion is found by evaluating the rate constant at two temperatures. The first solution assumes no temperature gradient, using $T=T_0$ to calculate the rate constant. The second solution uses $T=\langle T\rangle$ to calculate the rate constant, where $\langle T\rangle$ is the average temperature across the cross-section of a 2-D model as found using a two-point orthogonal collocation solution (Finlayson, 1980):

$$\langle T\rangle=\frac{\int_0^{2\pi}\int_0^1 T(r)r\,dr\,d\theta}{\int_0^{2\pi}\int_0^1 r\,dr\,d\theta}=\frac{\sum w_j T_j}{\frac{1}{2}}=\frac{3}{4}T_1+\frac{1}{4}T_2. \tag{24}$$

Orthogonal collocation applied to the boundary condition gives equations (25) and (26):

$$-\sum_{i=1}^{2} A_{2,i}T_i=Bi_w(T_2-T_w) \tag{25}$$

$$T_2=\frac{3T_1+Bi_w T_w}{3+Bi_w}. \tag{26}$$

Then, letting $T_1=T_0$ and combining equations (24) and (26) gives equation (27):

$$\langle T\rangle=\frac{3}{4}T_0+\frac{3T_0+Bi_w T_w}{12+4Bi_w}. \tag{27}$$

We then evaluate the outlet concentration twice using the reaction rate for each tempertature. We require the outlet concentrations to differ by less than 1%. Radial dispersion is neglected when equation (28) is satisfied:

$$1-\frac{0.01F_0}{\rho_B R_0 V}\leq\frac{k_1(T_0)}{k_2(\langle T\rangle)}\leq 1+\frac{0.01F_0}{\rho_B R_0 V}. \tag{28}$$

Notice that $k_1(T_0)=k_2(\langle T\rangle)$ if the wall temperature is equal to the inlet temperature, as in the case for the phythalic anhydride reactor. In that case, our criterion is inconclusive so the criterion from Mears (1971) is employed instead. This criterion predicts that at the hot-spot the average reaction rate at the cross-section will differ from the local reaction rate at the wall by less than 1% if equation (29) is satisfied:

$$1-\frac{0.4\lambda_{er}T_w}{(-\Delta H_{rxn})R_{a0}\gamma_w R_t^2}<\frac{4d_p}{Bi_w R_t}<1+\frac{0.4\lambda_{er}T_w}{(-\Delta H_{rxn})R_{a0}\gamma_w R_t^2}. \tag{29}$$

Note that this criterion is based on variations in reaction rates rather than in outlet concentrations. In other cases any appropriate two temperatures can be used in equation (28).

The criterion for axial dispersion is from Levenspiel and Bischoff (1963). For this criterion, the outlet concentration with axial dispersion will be within 1% of the outlet concentration without axial dispersion if equation (30) is satisfied:

$$\frac{d_p L}{Pe_{m,a}}<0.01\left(\frac{\rho_B R_0}{C_0 u_0}\right)^{-2}. \tag{30}$$

The values of the criteria for the three oxidation reactors are presented in Tables 5–7. If the value of the criterion falls between the lower and upper limits, then that phenomenon will not affect the outlet concentration by more than 1%. It should be noted that the values for the maleic anhydride reactor were not calculated at the inlet temperature. No

Table 5. Criterion results for the sulfur trioxide reactor

Phenomenon	Criterion value	Lower limit	Upper limit	Important?
Radial dispersion	0.13	0.996	1.004	Yes
Axial disperson	0.0024	0	4×10^{-7}	Yes
Heterogeneity	1.06	0.996	1.004	Yes
Density variations	1.38	0.996	1.004	Yes

Table 6. Criterion results for the phthalic anhydride reactor

Phenomenon	Criterion value	Lower limit	Upper limit	Important?
Radial dispersion	0.37	0.62	1.38	Yes
Axial dispersion	0.009	0	0.126	No
Heterogeneity	0.986	0.988	1.012	Maybe
Density variations	0.946	0.988	1.012	Yes

Table 7. Criterion results for the maleic anhydride reactor

Phenomenon	Criterion value	Lower limit	Upper limit	Important?
Radial dispersion	1.4	0.94	1.06	Yes
Axial dispersion	0.015	0	14.5	No
Heterogeneity	0.62	0.94	1.06	Yes
Density variations	0.69	0.94	1.06	Yes

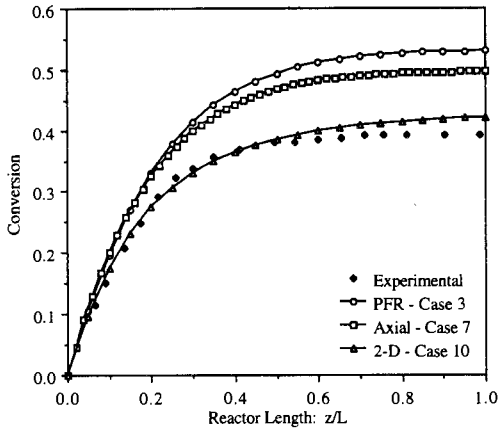

Fig. 1. Conversion for the sulfur trioxide reactor. Experimental data from Schuler *et al.* (1954).

reaction occurs at the inlet temperature. The reaction initiates at about 565 K, so the criterion values were calculated at this temperature.

SULFUR TRIOXIDE REACTOR

The 10 simulations outlined in Table 2 were run for the SO_2 reactor using CRDT. These simulations allow users to compare reactor type and the effect of the various transport phenomena. Figure 1 is a plot of the conversion of SO_2 vs the reactor length for various reactors, including experimental data from Schuler *et al.* (1954). Figure 2 shows the temperature as a function of reactor length for the three reactor types. The conversion and temperature are averaged across the reactor radius for the 2-D simulations. Experimental data for the temperature at the centerline agrees with the centerline temperature from the 2-D simulation but is not shown. Conversion in Simulation 3 is 26% higher than Simulation 10, showing the effect of a 2-D reactor. One would expect that the 2-D model will give

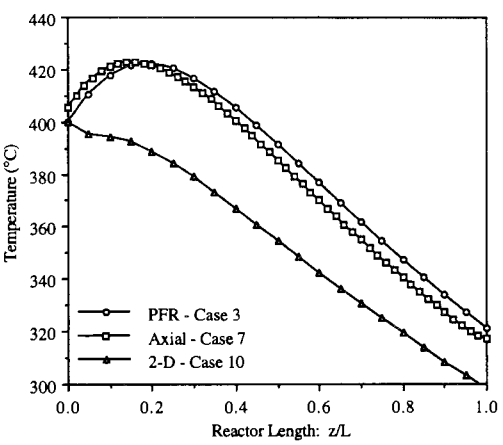

Fig. 2. Temperature profiles for sulfur trioxide reactor.

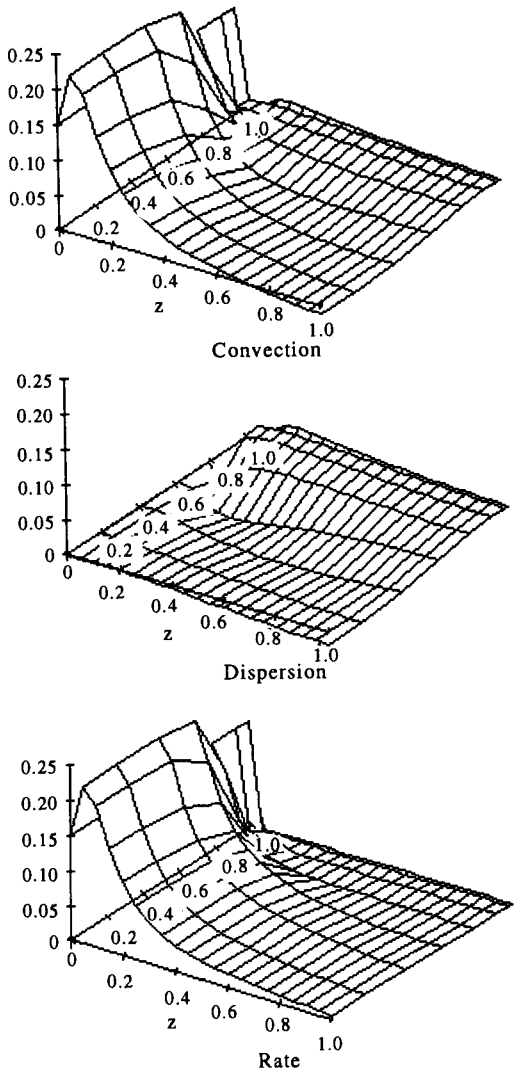

Fig. 3. Dispersion, convection, and rate terms for the sulfur trioxide mass balance.

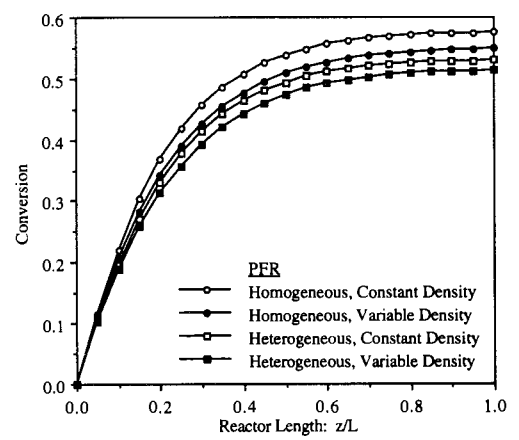

Fig. 4. Comparison of conversions for various effects in the sulfur trioxide reactor. Simulations 1–4.

Table 8. Importance of phenomena in sulfur trioxide reactor

Phenomenon	Literature	Criterion	CRDT
Radial dispersion	Yes	Yes	Yes
Axial dispersion	Yes	Yes	Yes
Heterogeneity	Yes	Yes	Yes
Density variations	No	Yes	Yes

different results than a 1-D model based on the high Biot number for this reactor. The significance of radial dispersion can be demonstrated further by comparing the magnitudes of the three terms in equation (6). Figure 3 presents a 3-D representation of the convection, dispersion, and rate terms. The z-axis represents the dimensionless magnitude of each term of the SO_3 mass balance equation. Note that the dispersion term is significant throughout the length of the reactor. Also, there are significant radial profiles in the convective and rate terms. Even though the radial dispersion term is only about 10% of the reaction rate term, it has an important effect on the conversion.

Figures 1 and 2 also suggest that axial dispersion may be important in this reactor. The conversion in Simulation 3 is 7% greater than the conversion from Simulation 7. The significance of axial dispersion in this reactor can be attributed to the reactor's short length. Notice that the curvature of the axial dispersion model closely follows the curvature of the experimental data. This suggests that a model including both axial dispersion and radial dispersion will represent the experimental data better than either of the individual models, as was confirmed by Young and Finlayson (1973).

Density and heterogeneous effects are studied using the PFR model, as shown in Fig. 4. Conversion of SO_2 is reduced by 8% when heterogeneous effects are included in the model. This suggests, along with the agreement of the experimental data with Simulation 10 in Fig. 1, that heterogeneous effects need to be accounted for in the model for this reactor.

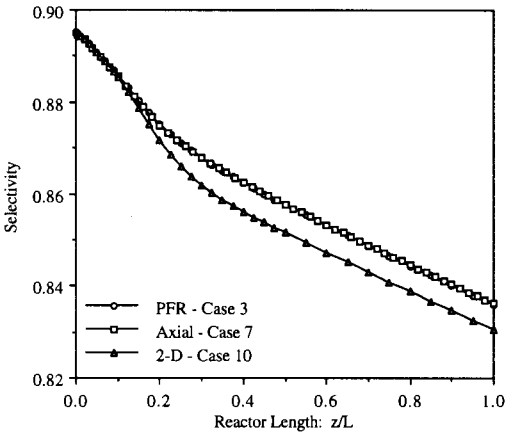

Fig. 6. Selectivity for the phthalic anhydride reactor.

Including density variations in the model reduce conversion of SO_2 by 5%. This result can be attributed to the large temperature difference between the inlet and wall temperatures. Mole changes owing to reaction magnify the effect. Pressure drop is negligible in this reactor due to the short length and a low Reynolds number. Including both density variation and heterogeneous effects in the model result in a 12% decrease in conversion of SO_2. Thus, the results of the simulations suggest that the appropriate model for this reactor would be a tubular-flow reactor including both axial dispersion and radial dispersion, heterogeneous effects, and density variations.

Table 8 compares the results from the simulations to the criteria's predictions and the models from the previous study. Recall that the concentration out of the reactor had to vary by more than 1% for the phenomena to be important enough to include in the model. The model used by Young and Finlayson

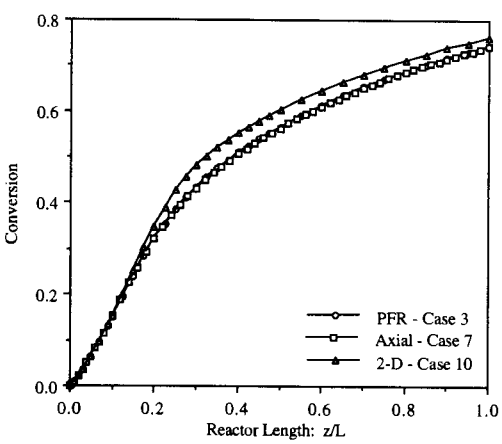

Fig. 5. Conversion for the phthalic anhydride reactor.

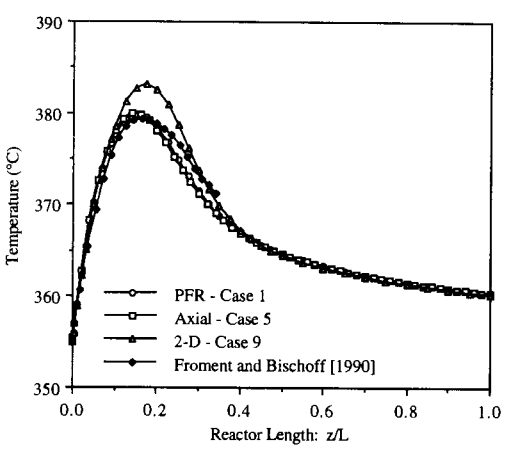

Fig. 7. Temperature profiles for the phthalic anhydride reactor.

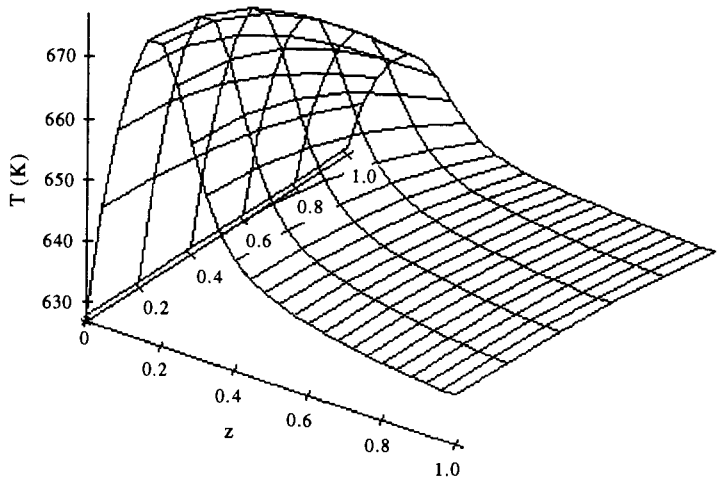

Fig. 8. Temperature profile in the *o*-xylene 2-D reactor.

included all the phenomena, except the total concentration was assumed constant. The criteria predicted all of the phenomena to be important, and the simulations done with CRDT agree with the predictions.

PHTHALIC ANHYDRIDE REACTOR

The 10 simulations were also performed by CRDT for the oxidation of *o*-xylene to phthalic anhydride. Figure 5 plots conversion of *o*-xylene against reactor length for the three reactor types. The conversion is 3% greater in the 2-D model than in the 1-D models. Selectivity is a better measure of the performance of the reactor because side reactions occur in this reaction system. Equation (31) defines the selectivity as the ratio of moles of desired product to the moles of reactant converted:

$$S = \frac{F_{PA}}{F_{PA} + F_{CO_2}}. \tag{31}$$

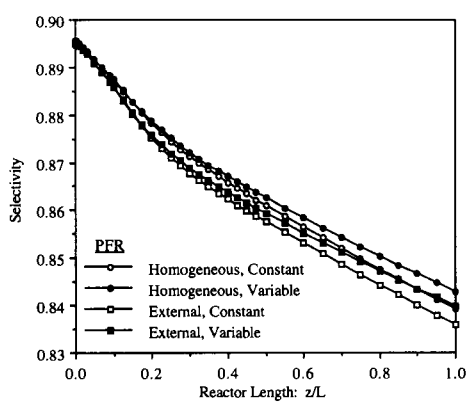

Fig. 9. Selectivity comparison for various effects in phthalic anhydride reactor. Simulations1–4.

Figures 6 and 7 show the selectivity and temperature profiles vs the reactor length for the three reactor types. Data from simulations performed by the previous investigators are also presented in Figure 7. The selectivity in Simulation 10 is less than 1% lower than in the 1-D simulations, although the average temperature in the 2-D simulation is greater at the hot-spot than the temperatures in Simulations 3 and 7. Thus, it can be concluded that axial dispersion and radial dispersion have no significant effect on the amount of phthalic anhydride produced in the reactor models. However, the 2-D model does show a significant radial temperature profile as can be seen in Fig. 8. This explains why the Mears criterion, equation (29), predicts that radial disperson is important. Radial dispersion does affect the temperature profile but its influence on conversion and selectivity is negligible.

Heterogeneity and density variations are studied using the PFR model. The selectivity for Simulations 1, 2, 3, and 4 is plotted vs reactor length in Fig. 9. Heterogeneity and density variations influence the selectivity by less than 1%. Notice that the two effects cancel each other; the simulation where both effects are included gives nearly the same profile as the simulation where neither was included. Thus, the simulations done with CRDT suggest that a simple plug-flow reactor model without heterogeneous effects and with the assumption of constant total concentration is sufficient to predict

Table 9. Importance of phenomena in phthalic anhydride reactor

Phenomenon	Literature	Criterion	CRDT
Radial dispersion	Yes	Yes	Yes
Axial disperson	No	No	No
Heterogeneity	No	Maybe	No
Density variations	No	Yes	No

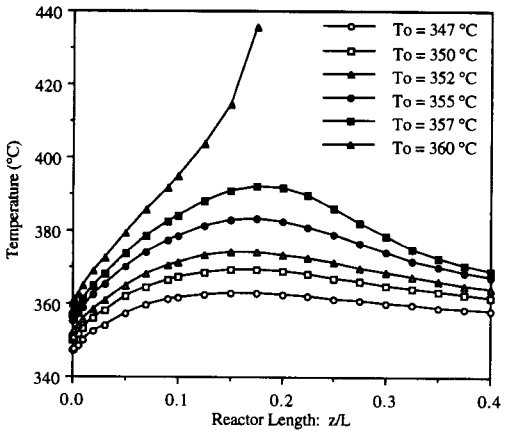

Fig. 10. Temperature profiles showing runaway in phthalic anhydride reactor.

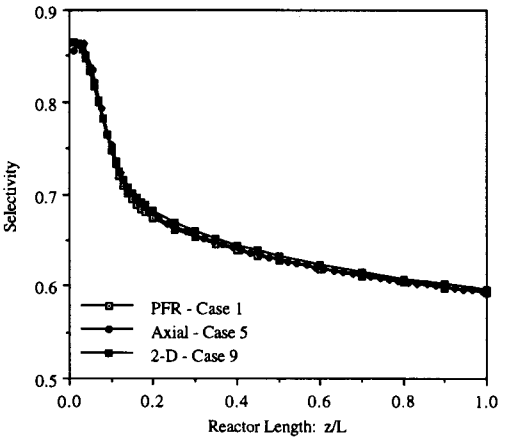

Fig. 12. Selectivity for the maleic anhydride reactor.

the amount of phthalic anhydride produced by this reactor. If an accurate measure of the temperature profile in the reactor is desired, then the 2-D model should be used.

The criteria's predictions are compared with the simulation results and literature model in Table 9. Recall that the criterion for radial dispersion for this reactor is based on the energy balance at the hot-spot rather than the conversion. Thus it is accurate in its prediction as demonstrated by Fig. 8. Froment and Bischoff (1990) also compare the 2-D model with a 1-D model and reach the same conclusions.

The criterion for heterogeneity is borderline. The criterion for density variations suggests that it will be an important phenomenon. The simulations show that both of these effects are unimportant, which illustrates the limitations of criteria that are derived based on simple models. If the limit on the criteria is increased to 5%, both of these phenomena are predicted to be insignificant.

Parametric sensitivity can also be studied using CRDT. Figure 10 demonstrates the influence of inlet temperature on the oxidation of *o*-xylene. Notice that runaway occurs at an inlet temperature of 360°C as predicted by Froment and Bischoff (1990). The dimensionless concentration of phthalic anhydride is shown in Fig. 11, which demonstrates that the solution can be found even after runaway has occurred.

MALEIC ANHYDRIDE REACTOR

The same 10 simulations from Table 3 were run for the maleic anhydride reactor model. The heterogeneous effects in this reactor are resistances internal to the catalyst. Selectivity for this reaction system is the amount of n-butane converted to

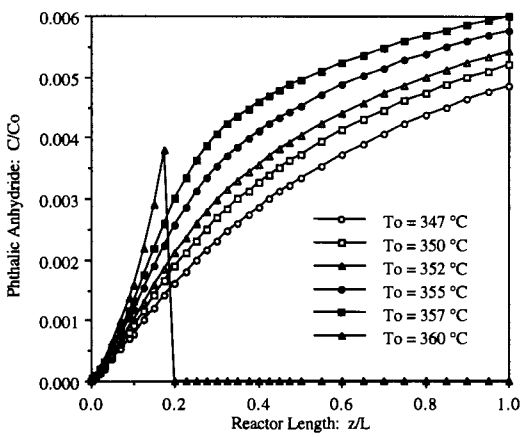

Fig. 11. Concentration profiles for runaway conditions in phthalic anhydride reactor.

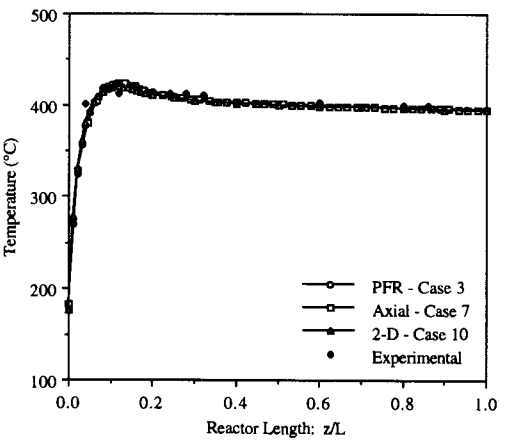

Fig. 13. Temperature profiles for maleic anhydride reactor. Experimental data from Sharma *et al.* (1991).

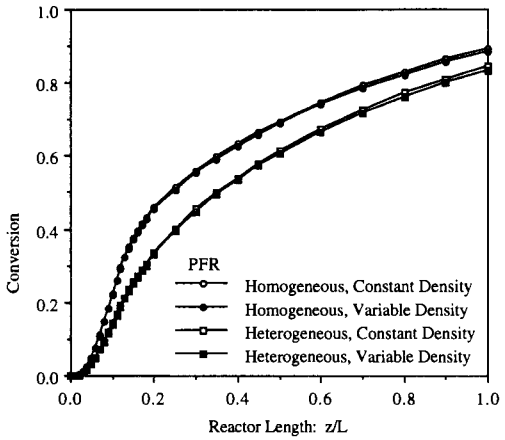

Fig. 14. Comparison of conversions for various effects in the maleic anhydride reactor. Simulations 1–4.

maleic anhydride and is plotted in Fig. 12:

$$S=\frac{F_{MA}}{F_{MA}+\frac{1}{4}(F_{CO}+F_{CO_2})}. \tag{32}$$

Figure 13 shows the temperature profiles in the reactor for the three reactor types along with experimental data from Sharma *et al.* (1991). From these two figures, it can be concluded that axial dispersion and radial dispersion have no significant infuence on the selectivity or temperature in the reactor. This is also true for conversion of reactant.

Figures 14 and 15 show the significance of heterogeneity and density variation on conversion and selectivity. Including heterogeneous effects reduced conversion by 6% and selectivity by 5% for the PFR model. Accounting for the variations in density resulted in a 1% reduction in conversion but a 2.5% increase in selectivity. This is caused by the pressure drop in the reactor. The ratio of the outlet pressure to the inlet pressure for this reactor is 0.65. With the

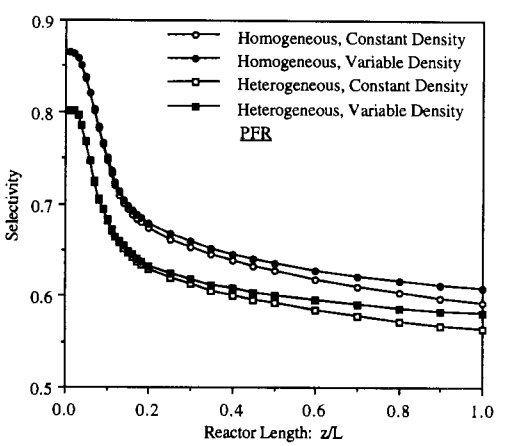

Fig. 15. Selectivity comparison for various effects in the maleic anhydride reactor. Simulations 1–4.

Table 10. Importance of phenomena in maleic anhydride reactor

Phenomenon	Literature	Criterion	CRDT
Radial dispersion	Maybe	Yes	No
Axial dispersion	No	No	No
Heterogeneity	Yes	Yes	Yes
Density variations	No	Yes	Yes

reduced pressure, the conversion will be preferential to the reaction producing the fewer number of moles, according to Le Chatelier's principle, and this is the desired reaction for this system.

Table 10 compares the results of the simulations done with CRDT to the criteria's predictions and the literature model. The previous investigators also suggested radial dispersion might be important in this reactor, but did not include it in their model. Figure 16 is a 3-D representation of the convection,

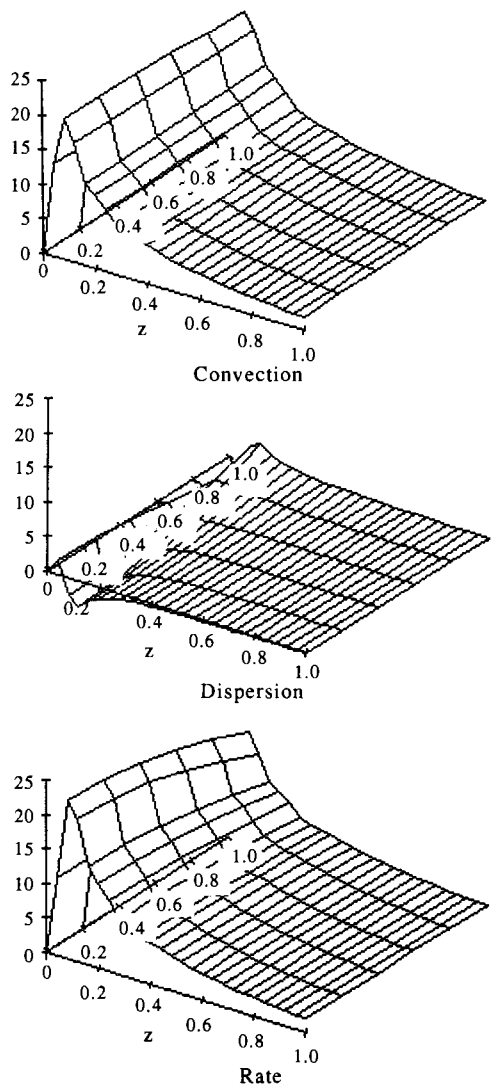

Fig. 16. Dispersion, convection, and rate terms for the maleic anhydride mass balance.

dispersion, and rate terms for this reactor. The dispersion term is significant at the reactor inlet but goes to zero partway downstream. This explains why there is little influence on the conversion or selectivity. The criterion predicts dispersion to be important because the criterion was calculated at the initiation temperature for this reactor. By contrast, Fig. 3 for the SO_2 reactor has a dispersion term that is non-zero throughout the reactor and the effect of radial dispersion is more important.

The results of the simulations for the maleic anhydride reactor suggest that a 1-D plug-flow model including heterogeneous effects and density variation is sufficient.

CONCLUSIONS

Three oxidation reactors were modeled and it was found that density variations are important for an accurate simulation. Radial dispersion, axial dispersion, and heterogeneity are important in some cases but not others. Criteria are developed to predict *a priori* which effects should be included. The Chemical Reactor Design Tool allows the inclusion of all the phenomena, and the criteria usually give results that agree with the numerical calculations.

Acknowledgement—The Chemical Reactor Design Tool was developed with partial support from the National Science Foundation.

NOMENCLATURE

a = Catalyst surface area/bed volume, /m
A_c = Cross-sectional area of reactor, m^2
$A_{2,i}$ = Collocation matrix
Bi = Biot number, $h_w/(\lambda_{er} R_t)$
C_j = Concentration of species j, kmol/m^3
C_{pj} = Specific heat of species j, kJ/(kmol K)
d_p = Particle diameter, m
d_t = Reactor diameter, m
Da_I = Damköhler number for mass, $\rho_B R_0 V/F_{tot}$
Da_{III} = Damköhler number for heat, $\rho_B R_0 V(-\Delta H_{rxn,1})/([\Sigma F_j C_{pj}]_0 T_{ref})$
D_{ea} = Effective axial dispersion coefficient, m^2/s
D_{er} = Effective radial dispersion coefficient, m^2/s
E = Activation energy, kJ/kmol
F_j = Molar flow rate, kmol/s
G = Mass flux, kg/(m^2 s)
h_p = Particle heat transfer coefficient, kJ/(m^2 s K)
h_w = Wall heat transfer coefficient, kJ/(m^2 s K)
$\Delta H_{rxn,i}$ = Heat of reaction for reaction i, kJ/kmol
k = First-order rate constants, s^{-1}
k_m = Particle mass transfer coefficient, m/s
L = Reactor length, m
P = Pressure, Pa
$Pe_{m,a}$ = Axial mass Peclet number, $u_0 d_p/(\varepsilon D_{ea})$
$Pe_{m,r}$ = Radial mass Peclet number, $u_0 d_p/(\varepsilon D_{er})$
$Pe_{m,L}$ = Axial mass Peclet number, $u_0 L/(\varepsilon D_{ea})$
$Pe_{h,L}$ = Axial heat Peclet number, $u_0 L[\Sigma F_j C_{pj}]_0/\lambda_{ea}$
$Pe_{h,r}$ = Radial heat Peclet number, $u_0 d_p[\Sigma F_j C_{pj}]_0/\lambda_{er}$
r_j = Rate expression for reaction i, kmol/kgcat s
R = Gas constant, kJ/kmol K
R_j = Reaction rate of species j, kmol/kgcat s
R_t = Radius of reactor, m
Re = Reynolds numbr, $\rho u_0 d_p/\mu$
S = Selectivity
St = Stanton number, $UL/(d_t G C_p)$
T = Temperature, K
u = Velocity, m/s
U = Heat transfer coefficient, kJ/(m^2 s K)
V = Reactor volume, m^3
w_j = Collocation matrix
X = $C_{SO_2}/C_{SO_2,0}$
y_{a0} = Mole fraction of limiting reactant

Greek symbols

ε = Void fraction in packed bed
ε_a = Mole change parameter
δ = Increase in the total number of moles per mole limiting reactant reacted
γ_w = E/RT_w
η = Effectiveness factor
λ_{ea} = Effective axial dispersion thermal conductivity, kJ/(m s K)
λ_{er} = Effective radial dispersion thermal conductivity, kJ/(m s K)
ν_{ji} = Stoichiometric coefficient of species j in reaction i
ν_j = Stoichiometric coefficient of species j
ν_a = Stoichiometric coefficient of limiting reactant
ρ = Density, kg/m^3
ρ_B = Bulk catalyst density, kg cat/m^3

Subscripts

oxy = *o*-Xylene
O_2 = Oxygen
pa = Phthalic anhydride
ma = Maleic anhydride
but = Butane

REFERENCES

Finlayson B. A., *Nonlinear Analysis in Chemical Engineering*. McGraw-Hill, New York (1980).

Finlayson B. A., B. M. Rosendall, G. Godfrey and S. Lee, *Chemical Reactor Design Tool, Student Manual and Textbook Supplement*. CACHE Corporation, Austin, Texas (1995a).

Finlayson B. A., B. M. Rosendall, G. Godfrey and S. Lee, *Chemical Reactor Design Tool, Instructor's Reference Manual*. CACHE Corporation, Austin, Texas (1995b).

Froment, G. F. and K. B. Bischoff, *Chemical Reactor Analysis and Design*, John Wiley & Sons, New York (1990).

Hindmarsh, A. C., *ODEPACK, A Systematized Collection of ODE Solvers, in Scientific Computing* (Edited by R. S. Stepleman *et al.*), p. 55. North-Holland, Amsterdam (1983).

Levenspiel O. and K. B. Bischoff, Patterns of flow in chemical process vessels. *Adv. chem. Engng* **4**, 95 (1963).

Mears D. E., Diagnostic criteria for heat transport limitations in fixed bed reactors. *J. Cat.* **20**, 127 (1971).

Seader J. D., Computer modeling of chemical processes. *AIChE Monogr. Ser., No. 15* **81**, 26 (1985).

Schuler , R. W., V. P. Stallings and J. M. Smith, Heat and mass transfer in fixed-bed reactors. *Chem. Engng Progr. Symp. Ser., No. 4* **48**, 19 (1954).

Sharma, R. K., D. L. Cresswell and E. J. Newson, Kinetics and fixed-bed reactor modeling of butane oxidation to maleic anhydride. *AIChE J.* **37**, 39 (1991).

Young, L. C. and B. A. Finlayson, Axial dispersion in nonisothermal packed bed chemical reactors. *Ind. Engng Chem. Fundam.* **12**, 412 (1973).